

Hideaki Shiraishi

Abstract

Magnetoencephalography (MEG) is one of the best ways to analyze neural function. In particular, MEG is valuable for assessing brain activity in children with epilepsy, because it is noninvasive and can be used multiple times for the same patient, thus enabling changes in epileptogenicity to be monitored as a child's growth.

Conventional MEG analysis is not always able to define the epileptogenic area. To this end, the single-dipole analysis tools can resolve localized epileptic MEG discharges and demonstrate equivalent current dipoles (ECDs) in cerebral cortex. However, diffuse or multifocal epileptic activities are not suitable for such ECD analyses, because the formula underpinning the single-dipole method assumes a circumscribed epileptogenic area. In this chapter, we discuss an alternative MEG tool whereby spatial filtering analysis is used for widespread or multifocal epileptogenic areas. Furthermore, we performed time-frequency analysis on a patient with symptomatic localization-related epilepsy who showed rhythmic activities as subclinical electrical discharges.

In conclusion, the single-dipole method, spatial filtering analysis, and time-frequency analysis could successfully resolve an epileptogenic area in patients with epilepsy. Thus, MEG analysis is potentially useful for presurgical evaluation or the diagnosis of epileptic syndromes for almost every patient with epilepsy.

Keywords

MEG • Epilepsy • Short-time Fourier transform • Dynamic statistical parametric mapping • Time-frequency analysis

H. Shiraishi, M.D., Ph.D. (✉)

Department of Pediatrics, Graduate School of Medicine, Hokkaido University, North 15, West 7, Kita-ku, Sapporo, Hokkaido 060-8638, Japan

e-mail: siraisi@med.hokudai.ac.jp

9.1 Introduction

Clinical applications of magnetoencephalography (MEG) should be expanded in the field of child epilepsy, first, because MEG can demonstrate valuable information about epileptogenicity noninvasively and, second, because a patient can undergo MEG multiple times to monitor changes in epileptogenicity during the child's growth.

MEG analysis is now established as an indispensable presurgical tool to evaluate candidates for epileptic surgery. In addition, MEG can also generate valuable information for the precise diagnosis of epileptic syndrome, though this application necessitates further development of appropriate methods of analysis to evaluate various kinds of epileptic activities.

In this chapter, we introduce a system of evaluating epileptic current in patients with epilepsy and further demonstrate the valuable role of MEG in this clinical field.

9.2 Methods

9.2.1 MEG Data Acquisition

MEG data were recorded using 204-channel helmet-shaped gradiometers (Vector View, Elekta AB, Stockholm, Sweden) at a 600-Hz sampling rate and then digitally filtered with a band-pass from 3 to 30 Hz for offline analysis. Segments containing abnormal paroxysms were identified manually.

9.2.2 Approach for Appropriate Analyses of Epileptic Current

ECD analysis is applicable for patients with localized epileptic foci, although this analysis is widely used and is available via preinstalled software in almost every MEG machine. In the first step of a MEG analysis or trial evaluation for epileptic spikes, ECD analysis is widely used because for the first screening of epileptic patients, we have to concentrate on the whole-brain MEG activity in a single view to select the most appropriate analysis method(s) for each patient. For localizing epileptiform activity, ECD analysis is applicable. Diffuse activity is not applicable for ECD analysis but for spatial filtering analysis, such as dynamic statistical parametric mapping (dSPM). Low-voltage fast activity, such as subclinical discharge or ictal activity, is not applicable for ECD analysis, since the signal to noise ratio is low. Time-frequency analysis can calculate the major gravity of distribution of the low-voltage oscillation and demonstrate the propagation of rhythmic activity.

9.2.3 Equivalent Current Dipole

Individual spikes were aligned on the basis of the peak latency and then analyzed. The distribution of brain activity generating the spikes was determined using a

source estimation approach, the equivalent current dipole (ECD) model. This model is appropriate when the underlying brain activity is focal, i.e., restricted to a relatively small region of the brain.

ECDs were calculated with xfit software (Elekta Neuromag Oy, Helsinki, Finland) using the single-dipole model. The conductivity geometry of the head was assumed to be spherical and symmetrical. Dipoles were calculated for each time-point measurement (every 2.5 ms) within 100 ms of each MEG spike. Results from all sensors were analyzed, with no regions of interest selected. The initial location for the iterative ECD fit was assumed to be under the sensor with the largest signal, and the ECD with the best goodness of fit (GOF) was selected as being representative of that particular MEG signal spike. The GOF is a measure of how well the ECD model explains the measured signals, and a dipole fit was accepted when the GOF was greater than 70 %. To visualize anatomical locations, the ECDs were superimposed on the magnetic resonance imaging (MRI) generated for each patient.

9.3 Direct Impact for Diagnosis of Epileptic Syndrome

Case 1: A 22-year-old boy with parietal lobe epilepsy (PLE). His seizures first occurred at the age of 8 years, beginning with sensory auras (tingling in the right hand) and evolving to right hemi-convulsion with his face and eyes deviated to the right side. His seizures have been precipitated by touch on the right side of his body and have occurred daily even with multiple antiepileptic drugs (AEDs). Initial scalp electroencephalography (EEG) screening detected no significant epileptiform discharges, and the patient was referred to our hospital. On performing MEG, we demonstrated remarkable spikes in the left parietal region with corresponding EEG spikes in the same area and ECDs accumulated in the postcentral gyrus (Fig. 9.1a). According to the clustering ECD location, this patient had a cortical lesion with a high signal on T2-weighted imaging (T2WI) in the vicinity of the central gyrus by MEG-guided MRI scanning (Fig. 9.1b). [18F]-Fluorodeoxyglucose positron emission tomography (FDG-PET) also showed glucose hypometabolism at the left postcentral gyrus. He could not attend junior high school for 3 years due to

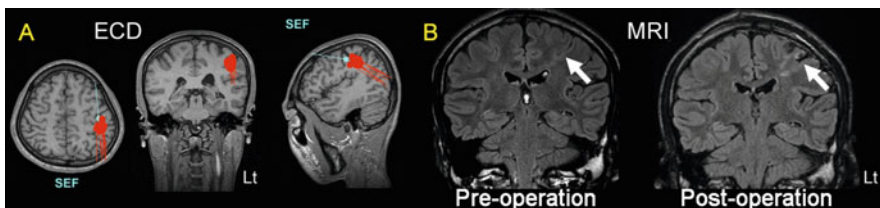


Fig. 9.1 (a) Equivalent current dipoles (ECDs) of MEG spikes were located in the posterior bank of the left central gyrus. The ECD of the somatosensory evoked field (SEF) localized the central gyrus. (b) MRI with FLAIR image showed a high signal at the bottom of the central gyrus and transmantle sign. Partial resection of the high-signal lesion was undertaken

recurrent complex partial seizures and secondary generalized seizures before the surgery. Furthermore, he was depressed by his disabled situation and prescribed antidepressant. Partial resection at the lesion stopped his complex partial seizure, but he retained abnormal sensation in the right upper arm (Fig. 9.1b). After his surgery, however, the patient showed improved mood and was able to attend and graduate from high school. His antidepressant prescription could be stopped, and he is currently working as a technologist in a company.

Case 2: A 17-year-old boy with atypical benign partial epilepsy (ABPE) in childhood. ABPE is characterized as childhood epilepsy with central-temporal EEG spikes and continuous spike and waves during sleep (CSWS). Patients with ABPE have multiple seizure types: focal motor seizures, atypical absence seizures, and myoclonic astatic seizures including epileptic negative myoclonus (ENM) but not tonic seizures [1]. Case 2 experienced his first seizure, a generalized tonic-clonic seizure, during sleep at the age of 3 years. His seizures occurred every 2–3 months, and he was treated with carbamazepine (CBZ) initially and up to the age of 7 years, when ENM occurred and the seizure frequency increased to more than 100 times every day. He was referred to our hospital at the age of 7 years. At this time, EEG showed CSWS, and MEG demonstrated concentrated spike sources at the peri-sylvian and peri-rolandic area (Fig. 9.2a). These findings and the patient's clinical course were consistent with the diagnostic criteria of ABPE [2]. His drug treatment was changed, with the CBZ replaced with ethosuximide (ESM), after which his ENM decreased dramatically. By the age of 14 years, his medication was stopped altogether, and the MEG spikes located unilaterally had disappeared by the age of 16 years (Fig. 9.2b, c). He currently shows normal intelligence and attends regular high school.

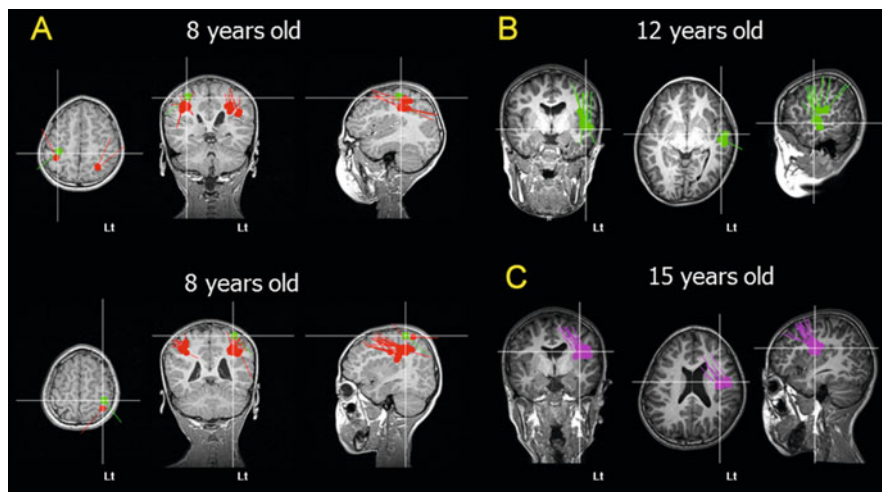


Fig. 9.2 (a) MEG showed concentrated MEG spike sources at the peri-sylvian and peri-rolandic areas bilaterally at the age of 8 years. (b) MEG spikes were located at the left side unilaterally at the age of 12 years. (c) MEG spikes were located at the left side unilaterally at the age of 15 years

9.3.1 Short-Time Fourier Transform Analysis

Short-time Fourier transform (STFT) analysis may be used to reveal the distribution of MEG polyspikes [15]. The MATLAB (MathWorks, Natick, USA) program was used to execute the STFT for the MEG signals in this study. Each signal was divided into small sequential frames, and fast Fourier transformation (FFT) applied to each frame.

In the present study, the STFT was implemented using a 256-point window at 426.7 ms per window (i.e., 256 points \times 1000 ms/600 Hz). The window was shifted every four points, corresponding to 6.7 ms (i.e., 1000 ms/600 Hz \times 4 points). The fast Fourier transform method was applied to each window. This process was repeated for all representative signals, and the time-frequency distributions were displayed as graphs.

Fast Fourier transform was performed for frequencies in the ranges of 3–30 Hz, 30–50 Hz, and 50–100 Hz. A signal's spectrum was considered to be aberrant when it was isolated from the background frequency spectrum on the graph. Such aberrant frequency spectra were superimposed onto the 3D-MRI reconstruction.

9.4 Direct Impact for Diagnosis of Epileptic Syndrome

Case 3: A 26-year-old woman with daily seizures. At the age of 2 months, she began to have spasms with bilateral upper limb contraction and head nodding, and her EEG showed hypsarrhythmia. She was diagnosed with West syndrome. After ACTH therapy, her seizures were initially resolved; however, they relapsed after a while. At the age of 2 years, she showed tonic posturing of the upper limbs and myoclonic seizures that were refractory to various AEDs (valproate, CBZ, clonazepam, phenobarbital, acetazolamide, and nitrazepam) as well as ketogenic diets. At the age of 17 years, her seizures became epileptic spasms with series of transform and tonic seizures. These seizures were symmetric from clinical findings, but her head deviated to the left occasionally. Her interictal EEG showed paroxysmal fast activities (PFAs) and bilateral frontal dominant diffuse spikes. Ictal EEG showed diffuse desynchronization in her seizures. At 19 years of age, 99mTc-ECD-SPECT showed hypoperfusion in the right frontal and temporal lobes dominantly. She was diagnosed with unclassifiable epilepsy.

At the age of 17 years, this patient underwent MEG analysis with PFA captured during the recordings. Although ECDs were located in bilateral hemispheres, most were scattered in the right parietal area (Fig. 9.3c). The MEG showed PFA corresponding to the EEG PFA in the right central-parietal-temporal area. Analysis of the PFA by STFT showed a significant power spectrum in the range from 10 to 25 Hz. The 3D-MRI moving image showed generation of PFA in the right angular gyrus that propagated contiguously to the postcentral gyrus and superior parietal lobule (Fig. 9.3a).

Ictal EEG and MEG of epileptic spasms were obtained simultaneously. STFT analysis before the onset of a clinical seizure showed a specific aberrant oscillation band of 10–18 Hz, although the EEG showed no specific findings. The 3D-MRI

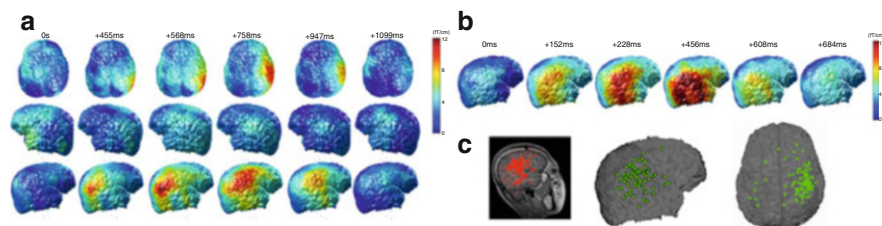


Fig. 9.3 (a) Analysis of PFA by STFT showed a significant power spectrum in the range from 10 to 25 Hz. The 3D-MRI moving image showed that PFA was generated in the right angular gyrus and propagated contiguously to the postcentral gyrus and superior parietal lobule. (b) In the ictal period, STFT analysis before the onset of a clinical seizure showed a specific, aberrant, 10–18-Hz oscillation band. The 3D-MRI moving image indicated that the specific oscillation band was generated in the right inferior parietal lobule. (c) Although ECDs were located in bilateral hemispheres, most ECDs were scattered in the right parietal area

moving image indicated that the specific oscillation band was generated in the right inferior parietal lobule, while analysis by STFT during the onset of a clinical seizure showed no specific aberrant oscillation. The high-power area of the PFA overlapped with that of the ictal paroxysmal discharge in the MEG (Fig. 9.3b).

The case was diagnosed and treated as cryptogenic-generalized epilepsy, suspected to be Lennox-Gastaut syndrome, and STFT analysis of the MEG demonstrated cryptogenic-localized epileptogenic foci in the right frontal and temporal lobes. STFT analysis also demonstrated the mechanism of the MEG rhythmic activity: the ictal discharges, providing the most useful information for the analysis of epileptogenic foci [3–5].

9.4.1 Dynamic Statistical Parametric Mapping (dSPM)

The dSPM method [6] is based on a noise-normalized minimum L2-norm estimate. For such analysis, we used an anatomically constrained distributed source model consisting of current dipole vectors located at each element; this model assumes the sources are located in the cerebral cortex. The cortical surface was segmented from the high-resolution MRI using FreeSurfer software [7, 8] and subsampled to about 2500 elements per hemisphere. For this estimate, the forward solution was calculated using a boundary element model (BEM) [9, 10] with conductivity boundaries determined from the segmented MRI. Only the inner surface of the skull is needed for MEG [10, 11].

The dSPM approach used to estimate the time course of activity at each cortical location is based on the generalized least-square or weighted minimum-norm solution [12, 13]; here, however, the estimate is normalized for noise sensitivity, thus providing a statistical parametric map [6] and reducing variation in the point-spread function between locations [14]. Simulations have suggested that the spatial resolution is 15 mm or better [6, 14]. Maps were calculated at 2.5-ms intervals. The significance of modulation at each site was calculated using an F-test [6, 15]. These

statistical maps differ from maps of estimated source strengths, since the estimated noise variance is not constant across different cortical locations. However, since the same noise covariance estimates are used at all time points for a given cortical location, source strength at a given location over time is directly proportional to the statistical map. The current approach thus provides dSPM of cortical activity, similar to the statistical maps typically generated using fMRI or PET data but with a millisecond temporal resolution.

9.5 Direct Impact for Diagnosis of Epileptic Syndrome

Case 4: A 21-year-old male patient with symptomatic/cryptogenic localization-related epilepsy with unclassifiable epileptic focus. He experienced drug-resistant recurrent seizures with impairment of consciousness from infancy. His EEG showed a bilateral diffuse spike and wave complex (Fig. 9.4). The paroxysm occurred frequently and was sometimes represented as rhythmic activity: subclinical

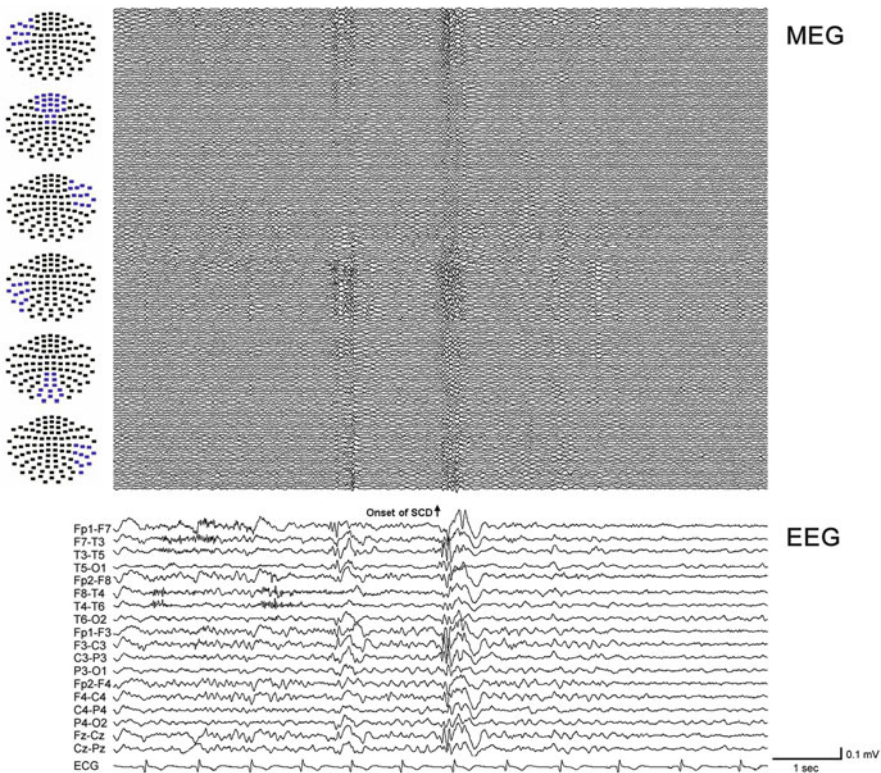


Fig. 9.4 Case 4, EEG and MEG. This patient's EEG showed a bilateral diffuse spike and wave complex. Paroxysm occurred frequently and sometimes represented as rhythmic activity: subclinical discharge. The MEG also showed bilateral diffuse spike activity

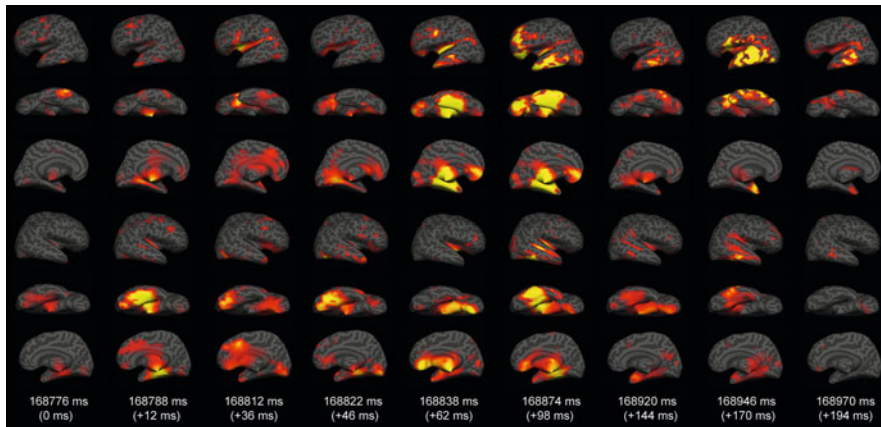


Fig. 9.5 Case 4, dSPM. dSPM demonstrated the change in spike activities at milliseconds resolution. The initial activity was generated in the left fusiform gyrus, propagated to the right cingulate gyrus and right fusiform gyrus (+12–46 ms), and moved to the left fusiform gyrus, middle and inferior temporal gyrus, and left superior frontal gyrus (+62–194 ms)

discharge. As for the EEG, his MEG showed bilateral diffuse spike activity (Fig. 9.4). ECD analysis could not resolve the epileptogenic focus, because the activity was not sufficiently localized to define the ideal single spike model. dSPM demonstrated the change in spike activities with milliseconds resolution: the initial activity was generated in the left fusiform gyrus, propagated to the right cingulate gyrus and right fusiform gyrus (+12–46 ms), and then moved to the left fusiform gyrus, middle and inferior temporal gyrus, and left superior frontal gyrus (+62–194 ms) (Fig. 9.5).

Due to the significant advantage of MEG over EEG in spatial resolution, MEG can show the evolution of epileptic current during the seizure. Furthermore, MEG study can be performed repeatedly, since it can be done noninvasively. This advantage is especially important for children.

Case 5: A 14-year-old patient with Lennox-Gastaut syndrome. He had tonic seizures and atypical absence seizures. His EEG and MEG showed diffuse slow spike and wave complex (Fig. 9.6). Gliosis was found at the marginal area circled by the middle and posterior cerebral arteries on diagnostic MRI. This lesion was probably related to asphyxia during the perinatal period. dSPM of the epileptiform discharges estimated the largest activation occurred during the spiking period in the right inferior frontal and superior temporal gyri and then suddenly propagated widely to the frontal and temporal lobes. The distribution of activity for the diffuse spike rhythm was wider than that for the diffuse spike and wave complex (Fig. 9.7a, c).

By using spatial filtering analysis, MEG studies are suitable for both localization-related and generalized epilepsy. MEG also has a significant advantage over EEG in spatial resolution, thus providing additional useful information in the diagnosis of epileptic syndromes.

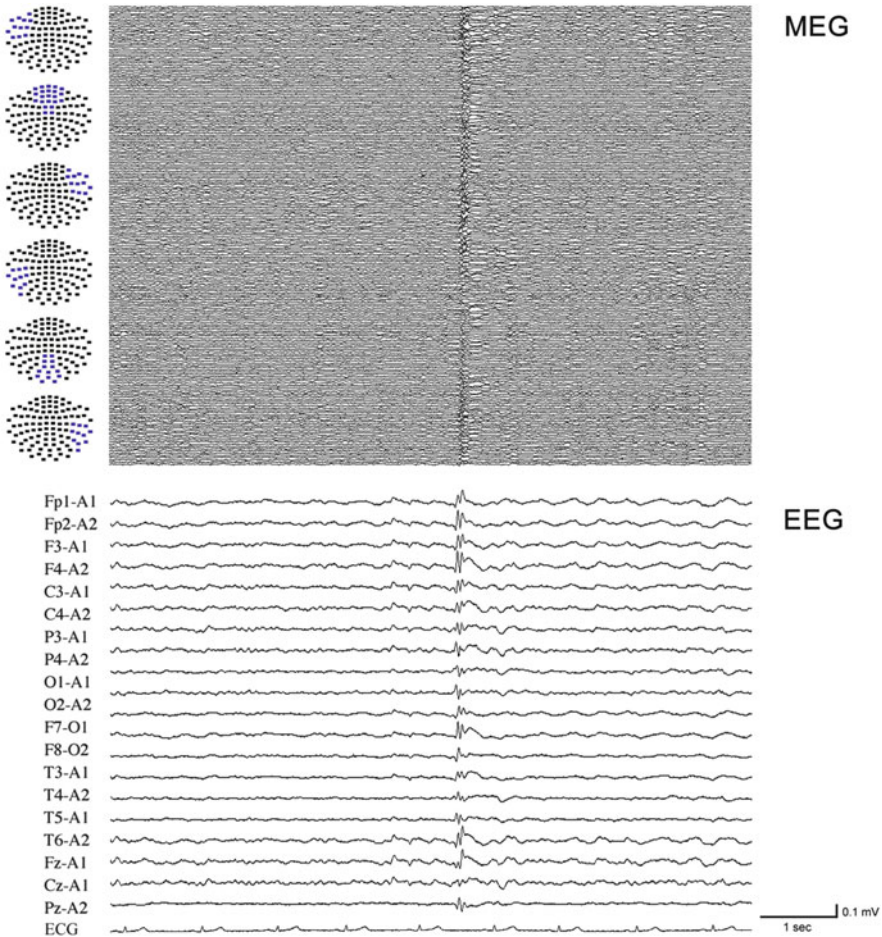


Fig. 9.6 Case 5, EEG and MEG. This patient’s EEG and MEG showed a diffuse slow spike and wave complex

9.6 For the Global Application of MEG for Every Patient with Epilepsy

We performed MEG analyses for 109 cases with epilepsy: 85 cases with symptomatic localization-related epilepsy (SLRE), five cases with symptomatic generalized epilepsy (SGE), 15 cases with idiopathic localization-related epilepsy (ILRE), two cases with idiopathic generalized epilepsy (IGE), and two cases with undetermined epilepsy (UDE). We initially performed single-dipole analysis for all cases, and the findings from 83 cases (65 cases with SLRE, 12 cases with ILRE, three cases with SGE, a case with IGE, two cases with UDE) were estimated as reasonable when

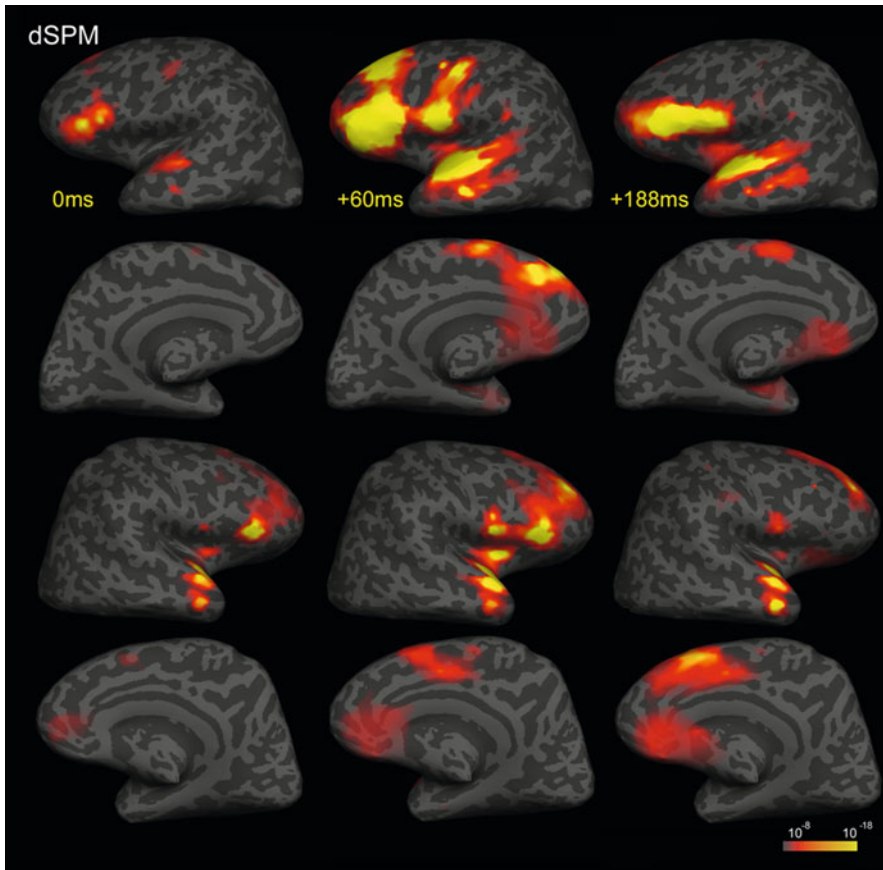


Fig. 9.7 Case 5, dSPM. dSPM of epileptiform discharges estimated the largest activation during the spiking period in the right inferior frontal and superior temporal gyri that then suddenly propagated widely to the frontal and temporal lobes. The distribution of activity for the diffuse spike rhythm was wider than that for the diffuse spike and wave complex

compared to their seizure manifestation and other electroclinical findings. We then used dSPM for the remaining cases, and 16 (ten cases with SLRE, three cases with ILRE, two cases with SGE, a case with IGE) could be evaluated reasonably. Finally, we applied SFT for the remaining ten cases, with reasonable findings achieved.

By using a combination of the single-dipole method, spatial filtering analysis, and time-frequency analysis, we successfully demonstrated the distribution of epileptogenic areas in patients with epilepsy. These findings suggested that MEG analysis could be useful for almost every patient with epilepsy during the presurgical evaluation and diagnosis of epileptic syndromes.

References

1. Aicardi J, Chevrie JJ. Atypical benign partial epilepsy of childhood. *Dev Med Child Neurol.* 1982;24:281–92.
2. Shiraishi H, Haginoya K, Nakagawa E, Saitoh S, Kaneko Y, Nakasato N, et al. Magnetoencephalography localizing spike sources of atypical benign partial epilepsy. *Brain Dev.* 2014;36:21–7.
3. Yagyu K, Takeuchi F, Shiraishi H, Nakane S, Sueda K, Asahina N, et al. The applications of time-frequency analyses to ictal magnetoencephalography in neocortical epilepsy. *Epilepsy Res.* 2010;90:199–206.
4. Sueda K, Takeuchi F, Shiraishi H, Nakane S, Asahina N, Kohsaka S, et al. MEG time-frequency analyses for pre- and post-surgical evaluation of patients with epileptic rhythmic fast activity. *Epilepsy Res.* 2010;88:100–7.
5. Sueda K, Takeuchi F, Shiraishi H, Nakane S, Sakurai K, Yagyu K, et al. Magnetoencephalographic analysis of paroxysmal fast activity in patients with epileptic spasms. *Epilepsy Res.* 2013;104:68–77.
6. Dale AM, Liu AK, Fischl BR, Buckner RL, Belliveau JW, Lewine JD, et al. Dynamic statistical parametric mapping: combining fMRI and MEG for high-resolution imaging of cortical activity. *Neuron.* 2000;26:55–67.
7. Dale AM, Fischl B, Sereno MI. Cortical surface-based analysis. I. Segmentation and surface reconstruction. *Neuroimage.* 1999;9:179–94.
8. Fischl B, Sereno MI, Tootell RB, Dale AM. High-resolution intersubject averaging and a coordinate system for the cortical surface. *Hum Brain Mapp.* 1999;8:272–84.
9. Oostendorp TF, van Oosterom A. Source parameter estimation in inhomogeneous volume conductors of arbitrary shape. *IEEE Trans Biomed Eng.* 1989;36:382–91.
10. Hämäläinen MS, Sarvas J. Realistic conductivity geometry model of the human head for interpretation of neuromagnetic data. *IEEE Trans Biomed Eng.* 1989;36:165–71.
11. Meijjs JW, Peters MJ. The EEG and MEG, using a model of eccentric spheres to describe the head. *IEEE Trans Biomed Eng.* 1987;34:913–20.
12. Hämäläinen MS, Ilmoniemi RJ. Interpreting magnetic fields of the brain: minimum norm estimates. *Med Biol Eng Comput.* 1994;32:35–42.
13. Dale AM, Sereno MI. Improved localization of cortical activity by combining EEG and MEG with MRI cortical surface reconstruction: a linear approach. *J Cogn Neurosci.* 1993;5:162–76.
14. Liu AK, Dale AM, Belliveau JW. Monte Carlo simulation studies of EEG and MEG localization accuracy. *Hum Brain Mapp.* 2002;16:47–62.
15. Dhond RP, Buckner RL, Dale AM, Marinkovic K, Halgren E. Spatiotemporal maps of brain activity underlying word generation and their modification during repetition priming. *J Neurosci.* 2001;21:3564–71.